


Cell-phone camera Raman spectrometer F

Cite as: Rev. Sci. Instrum. **92**, 054101 (2021); <https://doi.org/10.1063/5.0046281>

Submitted: 02 February 2021 . Accepted: 17 March 2021 . Published Online: 04 May 2021

 Dinesh Dhankhar,  Anushka Nagpal, and  Peter M. Rentzepis

COLLECTIONS

 This paper was selected as Featured



View Online



Export Citation



CrossMark

ARTICLES YOU MAY BE INTERESTED IN

[Non-contact and direct electrocaloric effect measurement for high-throughput material screening](#)



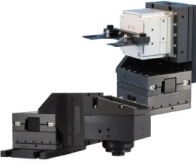
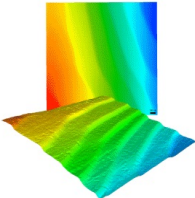
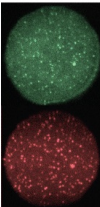
Review of Scientific Instruments **92**, 044902 (2021); <https://doi.org/10.1063/5.0044258>

[Broadband femtosecond spectroscopic ellipsometry](#)

Review of Scientific Instruments **92**, 033104 (2021); <https://doi.org/10.1063/5.0027219>

[Magnetic tweezers with magnetic flux density feedback control](#)

Review of Scientific Instruments **92**, 034101 (2021); <https://doi.org/10.1063/5.0039696>

 MCL MAD CITY LABS INC. www.madcitylabs.com	<p>Nanopositioning Systems</p> 	<p>Modular Motion Control</p> 	<p>AFM and NSOM Instruments</p> 	<p>Single Molecule Microscopes</p> 
---	--	--	---	--

Cell-phone camera Raman spectrometer

Cite as: Rev. Sci. Instrum. 92, 054101 (2021); doi: 10.1063/5.0046281

Submitted: 2 February 2021 • Accepted: 17 March 2021 •

Published Online: 4 May 2021



View Online



Export Citation



CrossMark

Dinesh Dhankhar,  Anushka Nagpal,  and Peter M. Rentzepis^{a)} 

AFFILIATIONS

Department of Electrical and Computer Engineering, Texas A & M University, College Station, Texas 77843, USA

^{a)} Author to whom correspondence should be addressed: prentzepis@tamu.edu

ABSTRACT

In this report, we describe the design, construction, and operation of a cell-phone-based Raman and emission spectral detector, which when coupled to a diffraction grating and cell-phone camera system provides means for the detection, recording, and identification of chemicals, drugs, and biological molecules, *in situ* by means of their Raman and fluorescence spectra. The newly constructed cell-phone spectrometer system was used to record Raman spectra from various chemicals and biological molecules including the resonance enhanced Raman spectra of carrots and bacteria. In addition, we present the quantitative analysis of alcohol-water Raman spectra, performed using our cell-phone spectrometer. The designed and constructed system was also used for constructing Raman images of the samples by utilizing a position scanning stage in conjunction with the system. This compact and portable system is well suited for *in situ* field applications of Raman and fluorescence spectroscopy and may also be an integrated feature of future cell-phones.

Published under license by AIP Publishing. <https://doi.org/10.1063/5.0046281>

I. INTRODUCTION

Cell-phone cameras allow one to record and store a picture within seconds. The compact cameras in modern day cell-phones are also increasingly becoming a par, even surpassing the quality and sensitivity of the traditional, stand-alone camera systems. This incredible advance in quality and low light sensitivity of cell-phone cameras is partly due to the use of back-illuminated CMOS sensors and advances in noise removal software pre-processing of the captured images. This outstanding quality and sensitivity of cameras in modern day cell-phones can also be utilized as sensitive light detectors for various types of sensing. There have already been several successful attempts to utilize cell-phone cameras as portable digital light microscope systems.¹⁻³ In addition, there are several cell-phone applications that can detect heart beats by analyzing the scattered light-emitting diode (LED) light from a finger placed over the camera lens. In previous communications,^{4,5} we described the design, construction, and operation of absorption and emission systems, which could be performed at remote areas, in order to detect and identify bacteria, pathogens, and molecules. In another previous communication,⁶ we utilized the compact monochrome CCD cameras, such as the ones used in the closed-circuit television (CCTV) cameras, to record the Ultraviolet (UV) fluorescence emitted from bacteria after excitation with Ultraviolet-C (UVC) LED light. We also correlated the damage inflicted, by Ultraviolet (UV) light, to the bacterial cells and the consequent decrease in the recorded

fluorescence intensity owing to bacterial death. UV fluorescence can also be used to detect extremely low concentrations of other fluorescing bio-molecules such as proteins and amino acids, tryptophan and tyrosine.

In this paper, we investigated the use of cameras used in modern day cell-phones in conjunction with advanced spectroscopic detection devices. The motivation for such applications was to use them as a means for utilizing the continuously improving camera sensitivity and picture quality of the modern day cell-phone camera for scientific purposes such as handheld cell-phone sized spectrometers, for the detection of pathogens and harmful chemicals through Raman and fluorescence spectroscopies, in remote areas and places where laboratory spectrometers are unavailable or cannot be used because of size and power requirements.

Raman and fluorescence spectroscopies are two powerful means for the detection and study of the structure and reaction mechanism of a molecule and biological species, such as proteins, amino and nucleic acids, and bacteria or viruses. These fast and non-invasive techniques based on scattering and emission of light provide a fingerprint of the molecule and its structure. Fluorescence spectroscopy is a very sensitive method for detecting the small concentrations of biological molecules, while the recorded Raman spectra provide a means for determining the vibrational modes of the molecule, under study, and, consequently, the structure of its molecular bonds. A combination of these techniques provides means for determining the characteristic structure(s) of complex

chemical and biological species. Raman spectroscopy may also be utilized for bio-molecules such as DNA and RNA, which either do not fluoresce or emit very low intensity fluorescence. Raman spectroscopy has also been utilized in numerous, diverse areas and applications, such as concentration of pharmaceutical drugs and other mixtures,^{7–10} determining the content of alcoholic fermentation in yeast¹¹ and solid fat content in milk;¹² determination of crystallinity of cellulose,¹³ identification of chemical isomers,^{14–16} and species concentration in cryogenic fuels for space industry¹⁷ are just a few of the applications of Raman spectroscopy. To that effect, several Raman instruments are utilized to identify drugs, harmful gases, and chemicals in the environment and industrial plants.^{18–21}

Raman spectroscopy has been applied for the detection and identification of biological molecules by excitation with ultraviolet and visible light in order to increase the signal intensity, thus generating enhanced resonance Raman spectra.^{22–27}

Several notable attempts have been made to build cost-effective Raman spectrometers;^{28–30} however, they still cost several thousands of USD, with the majority designed for laboratory-based experiments rather than for in-field testing. Our pocket sized designed and constructed Raman spectrometer system that utilizes right angle geometry to record Raman and resonance Raman spectra of molecules and biological species that contain colored pigments can be constructed for much lower cost (see Table I in the Appendix). The detector of our Raman device, described in this paper, was a cell-phone CCD/CMOS sensor camera, suggesting that this inexpensive pocket Raman system has the potential of being an integral part of ubiquitous cell-phones and thus makes possible the identification of chemicals and pathogens *in situ*, within minutes.

II. DESIGN AND CONSTRUCTION

Most commercial Raman spectrometers utilize backscattered geometry [Fig. 1(a)]; this geometry results in intense Raman spectra; however, they have the disadvantage of being difficult to remove the noise imposed by Rayleigh scattering and back reflected excitation light. To eliminate back reflected light, in this geometry, dichroic mirrors and expensive Rayleigh cutoff filters are required. In contrast, using the transmission form [Fig. 1(b)], even though the dichroic mirrors may be eliminated, the signal recorded is masked by the intense excitation laser line. Consequently, transmission Raman systems require high quality laser line

rejection filters and laser cleanup filters to eliminate excitation laser stray modes. One drawback of the Rayleigh rejection filters is that they may also limit the wavelength range in the low Raman shift regions ($<200\text{ cm}^{-1}$).

The design of our cell-phone-based Raman system presented in this paper utilizes a 90° excitation, and the geometry of the Raman signal collection is shown in Fig. 1(c). This cell-phone sized instrument reduces the intensity of Rayleigh scattering falling on the detector, resulting in an efficient removal of Rayleigh scattering. This right angle (90°) excitation geometry also has the advantage of being easier to use for the analysis of samples where a bulk property is to be measured, such as liquids or suspensions, vs microscopic level qualities. This is so since the scattering light collection optics can collect light from a wider collection area when it is in the right angle geometry. This would be especially effective when the excitation laser emits an intense collimated beam or a focused beam with a longer depth of focus. In this manner, the macroscopic size of the sample is interrogated by the laser beam, thereby providing an average Raman spectrum of the sample in the presence of microscopic heterogeneities. Low cost diode laser and simple plastic lenses were utilized for the construction of our excitation system. The design and construction are simple. The identification and detection of pathogens, such as colored bacteria, solvents, and even impurities in food are easily detected using our system.

Figure 2 displays a schematic representation of our cell-phone Raman spectrometer and Fig. 3 displays a photo of the constructed system with the major components marked. A diode laser, emitting at 532 nm and 50 mW, is used as the excitation source; other wavelength diode lasers may also be used. The laser excitation beam is focused onto the sample by means of a lens ($\sim 10\text{ mm}$ focal length and 4 mm diameter), and the Raman scatter light, from the sample, is collected by using a two-lens optical system, where the first lens collects and collimates the light, while the second focuses it with a matching f-number onto the spectrometer slit. The constructed spectrometer utilizes a transmission grating (1000 lines/mm), and a lens located inside the spectrometer collects and collimates the light onto the grating, thus increasing the intensity of the recorded spectra. It is interesting to note that this system operates effectively even without a collimating lens; however, the recorded Raman intensity is much lower.

III. MATERIAL AND METHODS

Most of the Raman spectra presented in this paper were acquired by using Google Pixel 3a (model XL) and Google pixel XL cell-phones. Our system also performed well using other cell-phones such as Nokia Lumina 1020 and Motorola Moto G. As mentioned earlier, a diode laser, emitting at 532 nm and 50 mW (model: 1875-532D-50-5V obtained from Laserland), was utilized as the light source for the scattered Raman spectra. The transmission grating that disperses the spectrum had a groove density of 1000 lines/mm and was obtained from Rainbow Symphony. The laser focusing lens, fluorescence collection lens, and focusing lens were all obtained from Laserland. The collimating lens used in the spectrometer was $\sim 25\text{ mm}$ in diameter, with a 60 mm focal length, and was obtained from Thorlabs. Raman spectra of common solvents such as ethanol, acetone, isopropyl alcohol, and methanol were recorded in a 1 cm path-length quartz cuvette. The cuvette was placed in front of the

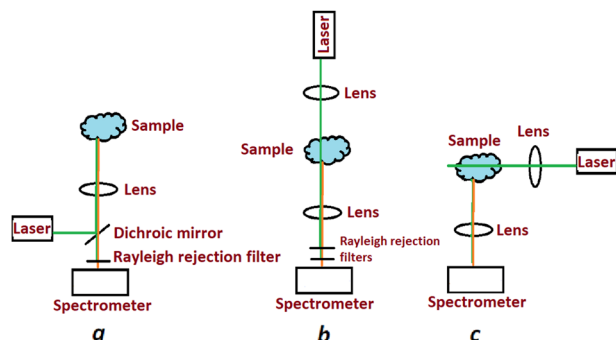


FIG. 1. Raman spectroscopy geometries: (a) backscattered geometry, (b) transmission geometry, and (c) right angle geometry.

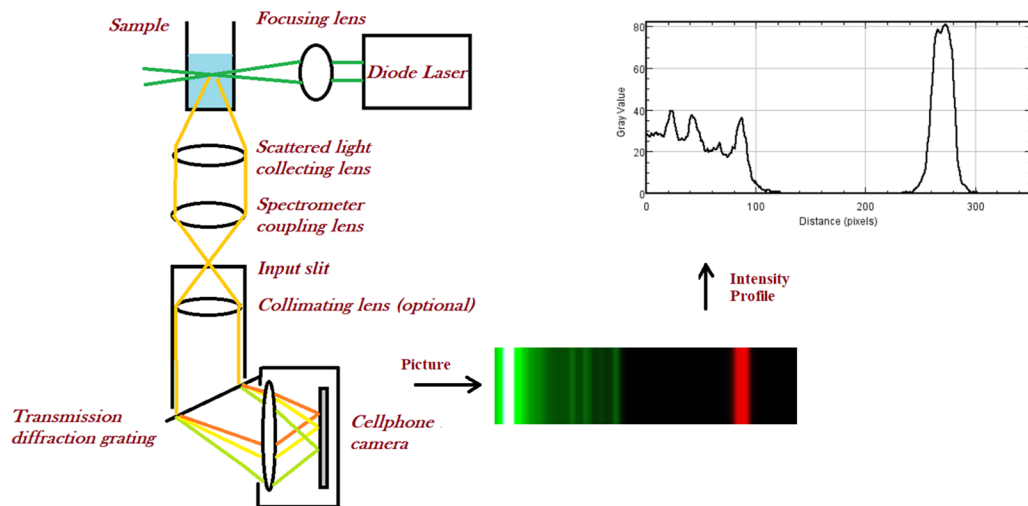


FIG. 2. Schematic diagram of the designed system.

focused excitation laser beam, and the emitted Raman spectra were recorded at right angle geometry, as shown in Fig. 2. For recording the Raman spectrum of opaque/solid objects, such as carrots and bacterial pellet, the sample was placed at the focal point at an angle of 45° to the incoming excitation laser beam, thereby directing the scattered Raman radiation toward the collection lens. A Rayleigh line cutoff filter was employed in all cases when Raman spectra of opaque objects were recorded. This Rayleigh filter was not normally utilized when the samples studied were clear and transparent.

A. Recording the Raman spectra

The cell-phone was placed behind the transmission grating with the camera directly facing the grating. Proper alignment of the camera was ensured by placing a cuvette filled with a dilute solution of Rhodamine 6G dye, as the sample, and recording its intense fluorescence spectrum dispersed by the transmission grating. The Rhodamine 6G solution cuvette is then replaced by a cuvette filled with the sample solution whose Raman spectrum has to be recorded. The Rayleigh scattered laser excitation light from the solution could

be seen with the cell-phone camera through the transmission grating. The autofocus mechanism in the cell-phone camera system was used in order to focus onto this Rayleigh scattered laser line, and the spectra were acquired in the night-sight mode. The night-side mode provides an exposure time of up to ~ 180 s by averaging several short exposures. Alternatively, other camera applications in the cell-phone such as the HD camera were also used. These applications allow for manual focusing, International Organization for Standardization (ISO) sensitivity of the camera, and exposure times up to a few seconds. Depending on the noise in the recorded spectra and lower acquisition times, spectra can be averaged to obtain a higher signal-to-noise ratio (SNR). For example, utilizing the HD camera app using the Google pixel XL smartphone, the maximum exposure time was limited to 0.7 s. In such a case, we acquired 20 spectra and averaged them in order to improve the signal-to-noise ratio.

For the case where a Rayleigh line cutoff filter is employed in the optical path, a highly scattering solution such as micro-particle suspension was utilized to detect weak Rayleigh scattered light through the cell-phone camera, and then, the detected light was focused onto the camera system. Once the proper focus is achieved, for spectrum acquisition, the micro-particle suspension can then be replaced with the sample.

B. Processing of the recorded spectra

The recorded spectra were rotated, when necessary, in order to vertically display all the spectral lines. The vertical axis of the spectra was binned by using the median value of all the pixels in the vertical axis, in order to remove noise (salt and pepper noise, hot pixels, and other noise) inherent in the acquired spectra. The resulting one-dimensional spectra (wavelength, λ vs intensity) were scaled in the vertical direction, and the spectral intensity was subsequently plotted vs wavenumber. The pixel to Raman shift wavenumber calibration was performed using the known Raman bands of ethanol. Spectral rotation, binning, scaling, and intensity profile plots were performed using the ImageJ software. Raman spectra were not corrected

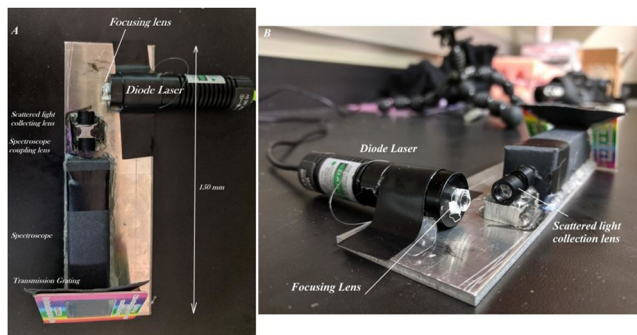


FIG. 3. Photo of the constructed system: top view (a) and side view (b).

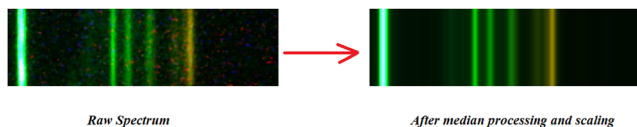


FIG. 4. Effect of spectral processing in removing the noise. The spectrum shown is the Raman spectrum of isopropanol in the fingerprint wavenumber region, acquired with our system.

for the variations of the quantum efficiency (intensity response) of the CMOS sensor as a function of the wavelength (instrument response correction). Figure 4 shows the effect of spectral processing in removing the noise.

The absorption spectra of samples, when required, were recorded by using a Shimadzu UV160 spectrophotometer. The carotenes were extracted from the raw carrots in the acetone solution. The HD camera app was utilized for recording the Raman spectra in order to determine the ethanol percentage in a water solution. Spectral acquisition time was 3.9 s, the ISO value was 7100, and the manual focusing function was employed to obtain proper focus.

IV. RESULTS AND DISCUSSION

A. Spectral resolution

The aperture of a cell-phone camera lens is ~ 2.5 mm. Even when the camera lens is placed directly in front of the grating, 2000 grooves are illuminated (1000 grooves per mm grating), making the resolving power, R value, of the system 2000. The theoretical resolution of the system is, thus, given by

$$\Delta\lambda = \lambda/R = 0.25 \text{ nm} \quad (1)$$

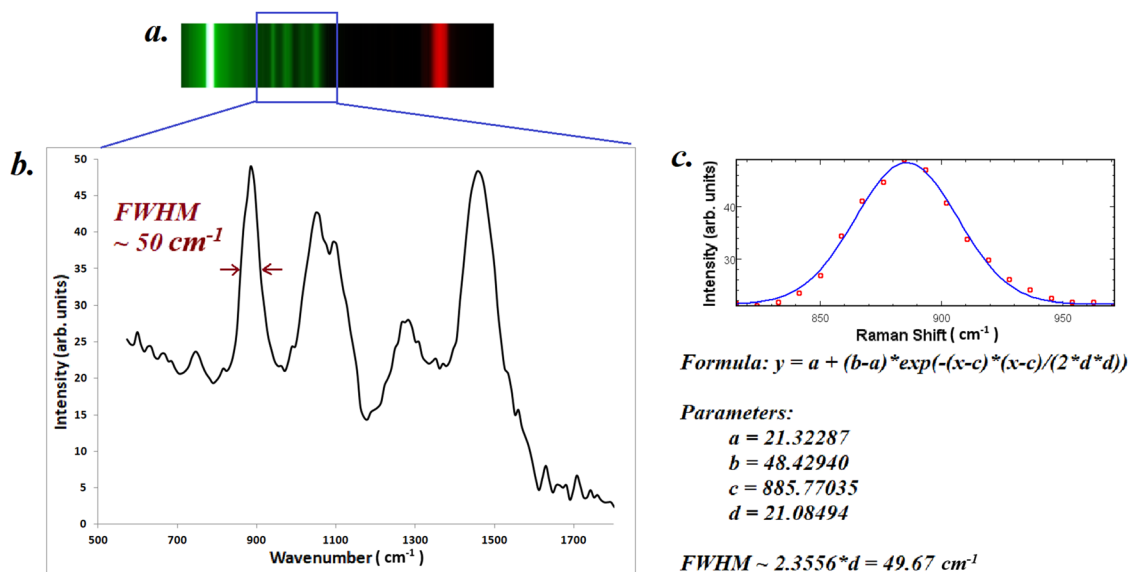


FIG. 5. Calculation of the resolution of the system with an ethanol Raman spectrum. Acquired Raman spectrum of ethanol (a), intensity plot of the fingerprint region of the ethanol Raman spectrum (b), and Gaussian fit of the 885 cm^{-1} Raman peak (c).

at 500 nm . The cell-phone camera consists of a 12 megapixel sensor. The dispersion of the spectrum on the sensor was $\sim 0.3 \text{ nm}$ per pixel. The resolution of the system is, however, limited by the input slit size, which should not be made too narrow because the amount of light reaching the transmission grating and subsequently to the cell-phone camera detector in the system is very small. In our optimum system, we obtained a spectral resolution $\sim 50 \text{ cm}^{-1}$, with $\sim 150 \mu\text{m}$ slit (Fig. 5).

In Fig. 5, the FWHM (Full Width at Half Maximum) was calculated by making a Gaussian fit,

$$y = Ae^{-\frac{(x-c)^2}{2\sigma^2}}, \quad (2)$$

using the 885 cm^{-1} peak of ethanol using ImageJ software. FWHM was then calculated as follows:

$$FWHM = 2\sigma\sqrt{2\ln 2} \quad (3)$$

$= 49.67 \text{ cm}^{-1}$, where σ is the standard deviation of the Gaussian fit.

B. Raman spectra

Typical Raman spectra of several organic molecules were recorded using the cell-phone Raman spectrometer, shown in Fig. 6. Figure 6(a) shows the processed spectra, from the pictures and Figs. 6(b)–6(d), which show the Raman spectra of ethanol, isopropyl alcohol, and methanol, respectively.

C. Resonance Raman spectra of biological molecules

The 532 nm excitation wavelength used for recording enhanced Raman spectra by our system is close to the absorption band of several common biological pigments such as carotenes (Fig. 7), which cause resonance enhancement³¹ of the Raman spectral intensities of the biological molecules that contain these pigments.

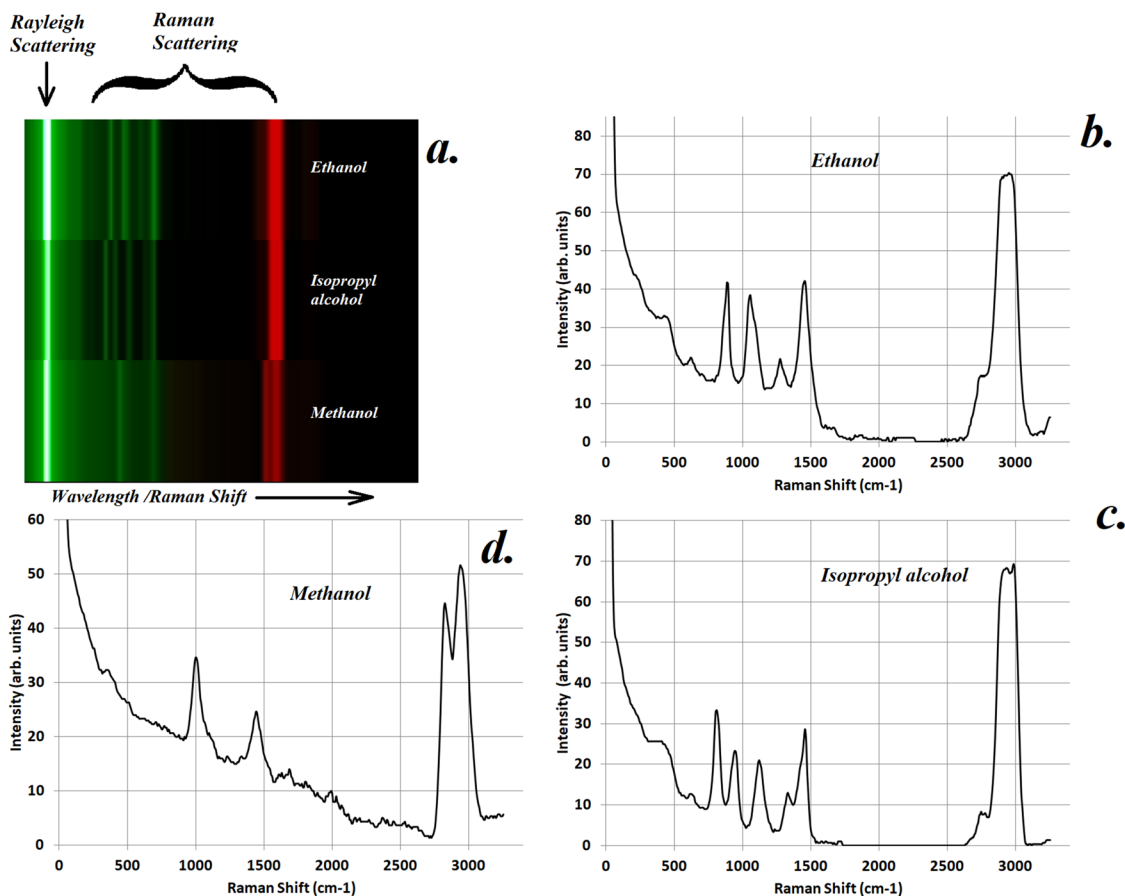


FIG. 6. Typical Raman spectra of different chemicals recorded by using the cell-phone Raman system: (a) processed spectra from the captured picture for ethanol, isopropyl alcohol, and methanol; (b)–(d) show the intensity plots of the Raman spectra of ethanol, isopropyl alcohol, and methanol.

The resonance enhanced Raman spectra of carrots recorded using the same cell-phone spectroscopic device is shown in Fig. 8. The carrot Raman spectra were converted from color to a monochrome image to avoid the intensity artifact on the fluorescence continuum due to transmission variances associated with the Red, Green, and Blue (RGB) Bayer filters used.

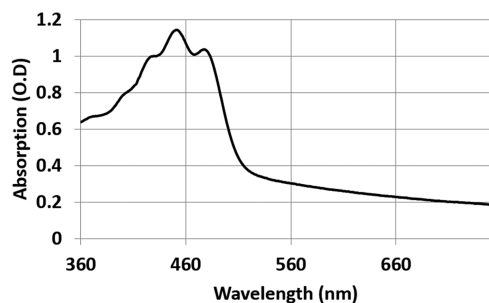


FIG. 7. Typical absorption spectrum of carotene pigments in carrot.

In addition, the Raman spectra of bacteria, such as *Micrococcus luteus* and *Serratia marcescens*, which contain color pigments that absorb in the 532 nm region, are shown in Fig. 9.

D. Quantitative analysis

In order to test for quantitative precision of this device, we measured the ratio of ethanol's 2935 cm^{-1} band to water's 3400 cm^{-1} band at various known concentrations of ethanol in water. Such determination is important when the ratio of active ingredients in consumer products is needed. The experimental data are shown in Fig. 10.

E. Recording Raman spectral images using a scanning stage

This novel system which we designed and described in this paper may also be used to record Raman spectra by scanning the sample in both the vertical and horizontal directions. The Raman spectra thus recorded display a linear Raman spectral image, which can be scanned in the vertical direction, thus providing a 2D Raman spectral image. Figure 11 shows the Raman spectral image of two

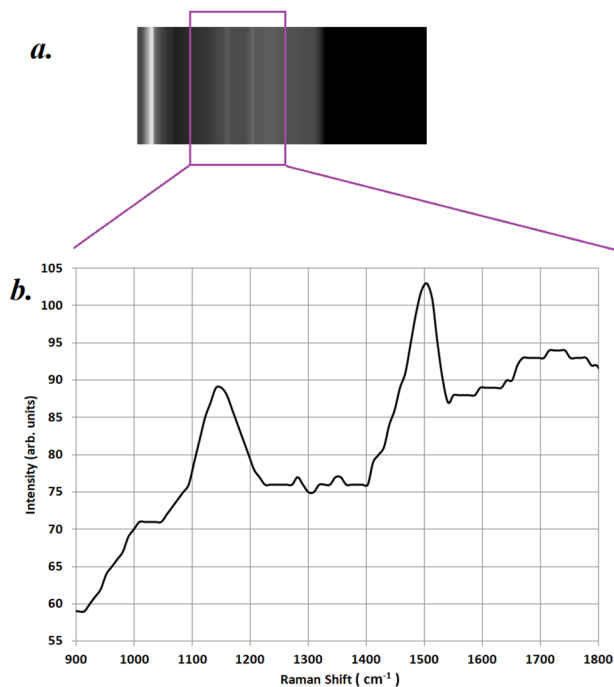


FIG. 8. Resonance enhanced Raman spectrum of carrots recorded by using our cell-phone system. The acquired spectrum (a) and the intensity plots showing prominent carotenoid bands associated with C=C stretching at $\sim 1500\text{ cm}^{-1}$ and C–C stretching at $\sim 1140\text{ cm}^{-1}$ (b).

cuvettes: one containing distilled water and the other ethanol placed next to each other. The water in red color is derived from the intensity of the water Raman band at 3400 cm^{-1} , whereas green color intensity corresponds to the ethanol Raman band at 2935 cm^{-1} .

F. Comparison of the cell-phone Raman and benchtop Raman systems' sensitivities

The cell-phone Raman spectrometer was compared to the HORIBA benchtop Raman spectrometer system (HORIBA XploRA), one of the most sensitive industrial Raman spectrometers, with distilled water as the test sample. The Signal-to-Noise Ratio (SNR) of the recorded Raman spectra was compared for the

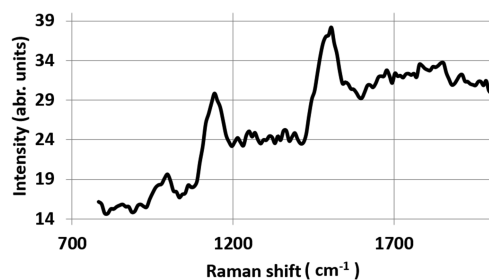


FIG. 9. Resonance enhanced Raman spectrum of *Serratia marcescens* recorded with our cell-phone spectroscopic device.

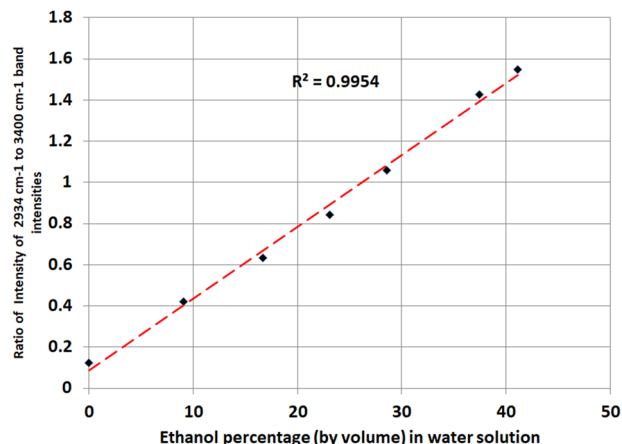


FIG. 10. Plot of the ratio of the 2950 cm^{-1} band of ethanol to the 3400 cm^{-1} Raman band of water as a function of ethanol percentage in water solution.

two instruments. The integration time for both the Horiba Raman spectrometer and cell-phone Raman spectrometer was set at 3.9 s. The grating selected in the HORIBA Raman spectrometer was 1200 lines/mm groove density, and the transmission grating in the cell-phone Raman spectrometer had a groove density of 1000 lines/mm. The excitation wavelength of both the spectrometers was 532 nm. The excitation power was 25 mW in the Horiba Raman system and 50 mW in the cell-phone Raman spectrometer. The spectrometer input slit was $200\text{ }\mu\text{m}$ in the Horiba Raman system, and it was $150\text{ }\mu\text{m}$ in the cell-phone Raman spectrometer. The excitation numerical aperture (NA) was 0.25 for Horiba and nearly the same for the cell-phone Raman spectrometer. The parameter chosen for the comparison was their Signal-to-Noise Ratio (SNR). The data of those experiments are shown in Fig. 12. The SNR of the Horiba system was roughly one order of magnitude better than the cell-phone system. We found that the SNR of the cell-phone system improves, nearly by a factor of 2, when a single RGB channel was used for analysis [Fig. 12(b)], Red (R) channel in this case. This is attributed to the fact that the Raman spectrum signal falls entirely in the red channel, and if we also include other channels, it results in the addition of noise from other channels, which does not contribute to the Raman signal. The noise depends, to a great extent, on the CCD/CMOS sensors used in the cell-phone cameras, which

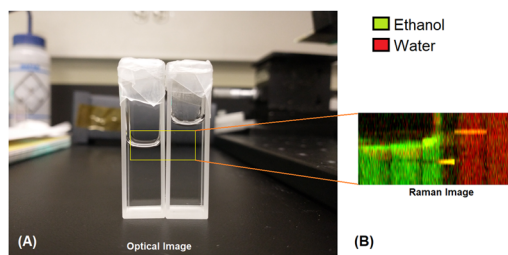


FIG. 11. Optical image (a) of two cuvettes containing ethanol and distilled water and the corresponding Raman image (b) of the scanned region on the right.

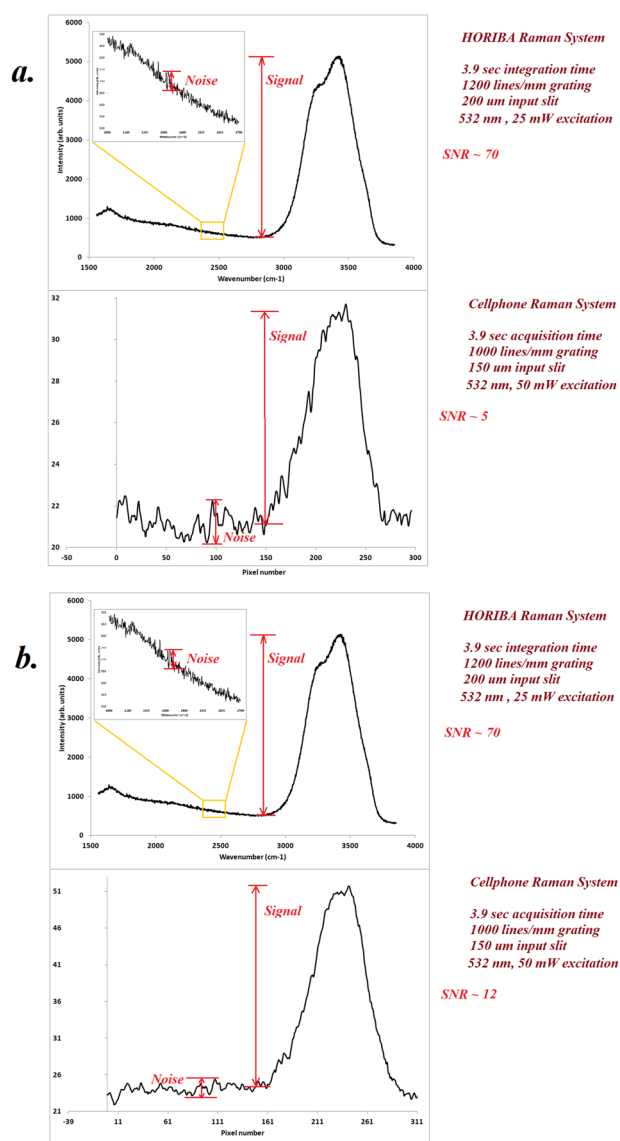


FIG. 12. Comparison of the Signal-to-Noise Ratio (SNR) for the water Raman spectrum obtained from the Horiba Raman spectrometer and cell-phone Raman spectrometer. (a) The comparison when intensities from all the three color channels, R, G, and B, are combined in the cell-phone camera Raman system and (b) when intensity of only the R channel (where the spectrum falls) is considered.

still suffer from large noise compared to the specialized CCD detectors utilized in the benchtop spectrometer instruments. This rather high noise in the cell-phone sensor may be attributed to the thermal factors (of uncooled detectors), small pixel sizes, and relative inferior CMOS sensors compared to specialized CCD sensors. Another contributing factor to the low intensity signal recorded by using the cell-phone instrument is the relatively lower diffraction efficiency of the transmission grating used in our cell-phone Raman spectrometer.

V. DISCUSSION AND CONCLUSION

In this study, we utilized cell-phone camera technology to record the Raman spectra of molecules, which provide a new, novel means for recording Raman, enhanced Raman, and other optical spectra, such as fluorescence. By recording the Raman spectra of biological molecules, this device provides a simple, reliable, and inexpensive method for the identification of molecules, bacteria, viruses, and other disease causing pathogens *in situ*. This instrument is intended to provide Raman and other spectral recording technologies as a commonplace for global positioning system (GPS) sensing or camera technology in a cell-phone.

The successful demonstration of the cell-phone camera-based Raman spectrometer system can be improved by eliminating several challenges in the cell-phone camera used as the spectroscopic sensor. Fortunately, most of these challenges can be rather easily overcome. One challenge was the fact that it is hard for lens-based systems to focus perfectly different wavelengths of light onto the image sensor. This effect might have played a role in degrading the spectral resolution of our system; however, this lack of tight focus was not noticeable, especially in the fingerprint region of the Raman spectra ($400\text{--}1800\text{ cm}^{-1}$). Small defocusing was observed in the red region of the spectrum; however, even there, the effect was not large enough to prevent the accurate identification of many chemical and biological species studied.

A second challenge is the rather limited dynamic range of the cell-phone captured images (8-bit per color channel). This limited dynamic range minimizes the simultaneous recording of strong and weak Raman lines. This problem can be overcome by using one of the several HDR (High Dynamic Range) camera applications, which enhance the dynamic range of the captured images by combining multiple images at different exposures.

A third possible challenge may be caused by using the red, green, and blue Bayer filters, which may distort the intensity profile of smooth continua. To overcome this problem, the image may be converted to a monochrome image by using an appropriate algorithm, which takes into account the spectral response of the individual Bayer filters.

In the cell-phone Raman spectroscopic system design, presented here, we simplified the excitation and emission geometry by using the minimum number of optical components for recording Raman spectra and their easy integration to modern cell-phone technology. This inexpensive yet accurate recording pocket Raman system has the potential of being an integral part of ubiquitous cell-phones that will make it possible to identify chemical impurities and pathogens, *in situ* within minutes.

ACKNOWLEDGMENTS

This work was supported, in part, by the Welch Foundation under Grant No. 1501928, the Air Force Office of Scientific Research under Grant No. FA9550-20-1-0139, and the Texas A & M Engineering Experiment Station (TEES). The authors would like to thank Professor Maria King for providing bacteria and valuable discussions.

APPENDIX: COST OF DIFFERENT COMPONENTS

TABLE I. Cost breakdown of various components for the design of the open access Raman spectroscopy system.

Component	Cost (USD)	Source
Diode laser, 532 nm, 50 mW	35	amazon.com
Small focusing and collimating lenses	10	amazon.com
Transmission grating	0.4	rainbowsymphonystore.com
Cardboard/glue/boxes, etc.	5	
Total	50.5 + cell-phone	

DATA AVAILABILITY

The data that support the findings of this study are available within the article.

REFERENCES

- H. Zhu and A. Ozcan, "Wide-field fluorescent microscopy and fluorescent imaging flow cytometry on a cell-phone," *J. Visualized Exp.* **174**, e50451 (2013).
- N. A. Switz, M. V. D'Ambrosio, and D. A. Fletcher, "Low-cost mobile phone microscopy with a reversed mobile phone camera lens," *PLoS One* **9**(5), e95330 (2014).
- C. W. Pirnstill and G. L. Coté, "Malaria diagnosis using a mobile phone polarized microscope," *Sci. Rep.* **5**(1), 13368 (2015).
- R. Li, U. Goswami, M. Walck, K. Khan, J. Chen, T. C. Cesario, and P. M. Rentzepis, "Hand-held synchronous scan spectrometer for *in situ* and immediate detection of live/dead bacteria ratio," *Rev. Sci. Instrum.* **88**(11), 114301 (2017).
- R. Li, U. Goswami, M. King, J. Chen, T. C. Cesario, and P. M. Rentzepis, "In situ detection of live-to-dead bacteria ratio after inactivation by means of synchronous fluorescence and PCA," *Proc. Natl. Acad. Sci. U. S. A.* **115**(4), 668–673 (2018).
- D. Dhankhar, R. Li, A. Nagpal, J. Chen, A. Krishnamoorthi, and P. M. Rentzepis, "A novel approach for remote detection of bacteria using simple charge-coupled device cameras and telescope," *Rev. Sci. Instrum.* **91**(7), 074106 (2020).
- C. J. Strachan, T. Rades, K. C. Gordon, and J. Rantanen, "Raman spectroscopy for quantitative analysis of pharmaceutical solids," *J. Pharm. Pharmacol.* **59**(2), 179–192 (2007).
- A. Heinz, M. Savolainen, T. Rades, and C. J. Strachan, "Quantifying ternary mixtures of different solid-state forms of indomethacin by Raman and near-infrared spectroscopy," *Eur. J. Pharm. Sci.* **32**(3), 182–192 (2007).
- L. Saerens, L. Dierickx, B. Lenain, C. Vervae, J. P. Remon, and T. D. Beer, "Raman spectroscopy for the in-line polymer–drug quantification and solid state characterization during a pharmaceutical hot-melt extrusion process," *Eur. J. Pharm. Biopharm.* **77**(1), 158–163 (2011).
- W. Gong, R. Shi, M. Chen, J. Qin, and X. Liu, "Quantification and monitoring the heat-induced formation of trans fatty acids in edible oils by Raman spectroscopy," *J. Food Measurement and Characterization.* **13**, 2203–2210 (2019).
- A. Picard, I. Daniel, G. Montagnac, and P. Oger, "In situ monitoring by quantitative Raman spectroscopy of alcoholic fermentation by *Saccharomyces cerevisiae* under high pressure," *Extremophiles* **11**(3), 445–452 (2007).
- C. M. McGoverin, A. S. S. Clark, S. E. Holroyd, and K. C. Gordon, "Raman spectroscopic prediction of the solid fat content of New Zealand anhydrous milk fat," *Anal. Methods* **1**(1), 29–38 (2009).
- U. P. Agarwal, R. S. Reiner, and S. A. Ralph, "Cellulose I crystallinity determination using FT–Raman spectroscopy: Univariate and multivariate methods," *Cellulose* **17**(4), 721–733 (2010).
- S. Mahapatra, Y. Ning, J. F. Schultz, L. Li, J.-L. Zhang, and N. Jiang, "Angstrom scale chemical analysis of metal supported *trans*- and *cis*-regioisomers by ultrahigh vacuum tip-enhanced Raman mapping," *Nano Lett.* **19**(5), 3267–3272 (2019).
- G. F. Bailey and R. J. Horvat, "Raman spectroscopic analysis of the *cis/trans* isomer composition of edible vegetable oils," *J. Am. Oil Chem. Soc.* **49**(8), 494–498 (1972).
- G. L. Johnson, R. M. Machado, K. G. Freidl, M. L. Achenbach, P. J. Clark, and S. K. Reidy, "Evaluation of Raman spectroscopy for determining *cis* and *trans* isomers in partially hydrogenated soybean oil," *Org. Process Res. Dev.* **6**(5), 637–644 (2002).
- V. S. Tiwari, R. R. Kalluru, F. Y. Yueh, J. P. Singh, W. S. Cyr, and S. K. Khijwania, "Fiber optic Raman sensor to monitor the concentration ratio of nitrogen and oxygen in a cryogenic mixture," *Appl. Opt.* **46**(16), 3345–3351 (2007).
- L. Harper, J. Powell, and E. M. Pijl, "An overview of forensic drug testing methods and their suitability for harm reduction point-of-care services," *Harm Reduct. J.* **14**(1), 52 (2017).
- K. Dégardin, A. Guillemin, and Y. Roggo, "Comprehensive study of a hand-held Raman spectrometer for the analysis of counterfeits of solid-dosage form medicines," *J. Spectrosc.* **2017**, 3154035.
- P. C. Kumar and J. A. Wehrmeyer, "Stack gas pollutant detection using laser Raman spectroscopy," *Appl. Spectrosc.* **51**(6), 849–855 (1997).
- T. T. X. Ong, E. W. Blanch, and O. A. H. Jones, "Surface enhanced Raman spectroscopy in environmental analysis, monitoring and assessment," *Sci. Total Environ.* **720**, 137601 (2020).
- K. A. Britton, R. A. Dalterio, W. H. Nelson, D. Britt, and J. F. Sperry, "Ultraviolet resonance Raman spectra of *Escherichia Coli* with 222.5–251.0 nm pulsed laser excitation," *Appl. Spectrosc.* **42**(5), 782–788 (1988).
- C. R. Johnson, M. Ludwig, S. O'Donnell, and S. A. Asher, "UV resonance Raman spectroscopy of the aromatic amino acids and myoglobin," *J. Am. Chem. Soc.* **106**(17), 5008–5010 (1984).
- Y. C. Cao, R. Jin, and C. A. Mirkin, "Nanoparticles with Raman spectroscopic fingerprints for DNA and RNA detection," *Science* **297**(5586), 1536–1540 (2002).
- J. M. Benevides, S. A. Overman, and G. J. Thomas, Jr., "Raman, polarized Raman and ultraviolet resonance Raman spectroscopy of nucleic acids and their complexes," *J. Raman Spectrosc.* **36**(4), 279–299 (2005).
- B. Lorenz, C. Wichmann, S. Stöckel, P. Rösch, and J. Popp, "Cultivation-free Raman spectroscopic investigations of bacteria," *Trends Microbiol.* **25**(5), 413–424 (2017).
- R. Li, D. Dhankhar, J. Chen, A. Krishnamoorthi, T. C. Cesario, and P. M. Rentzepis, "Identification of live and dead bacteria: A Raman spectroscopic study," *IEEE Access* **7**, 23549–23559 (2019).
- A. Arbildo L., E. H. Montoya R., and O. R. Baltuano E., "A homemade cost effective Raman spectrometer with high performance," *J. Lab. Chem. Educ.* **3**(4), 67–75 (2015).
- W. R. C. Somerville, E. C. Le Ru, P. T. Northcote, and P. G. Etchegoin, "High performance Raman spectroscopy with simple optical components," *Am. J. Phys.* **78**(7), 671–677 (2010).
- C. Mohr, C. L. Spencer, and M. Hippler, "Inexpensive Raman spectrometer for undergraduate and graduate experiments and research," *J. Chem. Educ.* **87**(3), 326–330 (2010).
- D. P. Strommen and K. Nakamoto, "Resonance Raman spectroscopy," *J. Chem. Educ.* **54**(8), 474 (1977).